A EUROPEAN JOURNAL OF CHEMICAL BIOLOGY

CHEMBIOCHEM

SYNTHETIC BIOLOGY & BIO-NANOTECHNOLOGY

Accepted Article

Title: Manipulating Active Structure and Function of Cationic Antimicrobial Peptide CM15 by the Polysulfonated Drug Suramin: A Step Closer to in vivo Complexity

Authors: Mayra Quemé-Peña, Tünde Juhász, Judith Mihály, Imola Csilla Szigyártó, Kata Horváti, Szilvia Bősze, Judit Henczkó, Bernadett Pályi, Csaba Németh, Zoltán Varga, Ferenc Zsila, and Tamás Beke-Somfai

To be cited as: *ChemBioChem* 10.1002/cbic.201800801

Link to VoR: http://dx.doi.org/10.1002/cbic.201800801

A Journal of

ChemPubSoc Europe

WILEY-VCH

www.chembiochem.org

10.1002/cbic.201800801

Manipulating Active Structure and Function of Cationic Antimicrobial Peptide CM15 by the Polysulfonated Drug Suramin: A Step Closer to *in vivo* Complexity

Mayra Quemé-Peña,[a] Tünde Juhász,[a]* Judith Mihály,[a] Imola Cs. Szigyártó,[a] Kata Horváti,[b] Szilvia Bősze, [b] Judit Henczkó, [c] Bernadett Pályi,[c] Csaba Németh,[a] Zoltán Varga,[a] Ferenc Zsila,[a] and Tamás Beke-Somfai,[a]*

[a] *Mayra Quemé-Peña, Dr. Tünde Juhász, Dr. Imola Cs. Szigyártó , Dr. Judith Mihály, Csaba Németh, Dr. Zoltán Varga, Dr. Ferenc Zsila, Dr. Tamás Beke-Somfai*
Institute of Materials and Environmental Chemistry, Research Centre for Natural Sciences, Hungarian Academy of Sciences
H-1117 Budapest, Magyar tudósok körútja 2, Hungary
E-mail: beke-somfai.tamas@ttk.mta.hu, juhasz.tunde@ttk.mta.hu

[b] *Dr. Kata Horváti , Dr. Szilvia Bősze*
MTA-ELTE Research Group of Peptide Chemistry, Hungarian Academy of Sciences, Eötvös Loránd University
H-1117 Budapest, Pázmány Péter sétány 1/A, Hungary

[c] *Judit Henczkó, Bernadett Pályi*
National Biosafety Laboratory, National Public Health Center
H-1097 Budapest, Albert Flórián út 2, Hungary

ABSTRACT

Antimicrobial peptides (AMPs) kill bacteria by targeting their membranes *via* various mechanisms involving peptide assembly often coupled with disorder-to-order structural transition. However, similar conformational changes were recently reported for several AMPs, where small organic molecules of both endogenous and exogenous origin induced folded peptide conformation. Thus, function of AMPs and natural host defense peptides can be significantly affected by the local complex molecular environment *in vivo*, nonetheless this area is hardly explored. To address the relevance of such interactions on structure and function, herein we tested the effect of the therapeutic drug suramin on the membrane activity and antibacterial efficiency of a potent hybrid AMP, CM15. Results provided insight to a dynamic system where peptide interaction with lipid bilayers is interfered with the competitive binding of CM15 to suramin, resulting in an equilibrium dependent on peptide-to-drug ratio and vesicle surface charge. *In vitro* bacterial tests show that when CM15-suramin complex formation dominates over membrane binding, antimicrobial activity is abolished. Based on this case study, it is proposed that small molecule secondary structure regulators can modify AMP function, which should be considered and could potentially be exploited in future development of AMP-based antimicrobial agents.

Key words: antimicrobial peptide, circular dichroism, folding, IR spectroscopy, suramin

INTRODUCTION

Antibiotic resistance has reached alarming levels and represents one of the biggest current global threats to health.[1] There is an urgent need for new antimicrobial agents that allows us to tackle this problem in innovative ways. Antimicrobial peptides (AMPs) have been identified as important leads for the next generation of antibiotics.[1b, 2] The significant advantage of AMPs resides in the global mechanism of their action, which is remarkably different from that of conventional antibiotics.[1d] AMPs display multifunctional properties with implications as potential therapeutic agents as they form an essential part of the innate immunity.[3] They exhibit rapid killing, and a broad spectrum of activity against a large array of microorganisms including Gram-positive and Gram-negative bacteria, fungi, protozoan and metazoan parasites.[1b, 4]

The unique and diverse group of AMPs are divided into several subgroups on the basis of amino acid composition and structure.[1c, 4c] Linear, cationic AMPs display a number of common characteristics including low molecular weight (10-50 amino acids) and amphiphilicity. The latter arises from the high content of positively charged (generally from +2 to +9) amino acids (lysine, arginine) along with a substantial proportion of hydrophobic residues (≥30%).[2b, 5] All of these are key structural features that guide the antimicrobial effects of these peptides.

The electrostatic repulsion between the charged side chains renders the solution structure of the majority of cationic AMPs intrinsically disordered (ID) with no discernible secondary structure.[1c, 5a, 6] Upon membrane binding, unstructured AMPs undergo a conformational change and fold into a well-ordered, mostly α-helical structure.[7] As these peptides exert their action within membrane environment, the membrane-associated conformational transition is believed as a crucial step in mediating their biological activities. This structural transition could also be dependent on the lipid composition leading to increased specificity towards membranes enriched in negatively charged

species.[1d, 8] However, the *in vivo* action of these peptides can be considered as a complex issue possibly including numerous types of interactions with small molecule agents. Indeed, previous studies in our group have suggested that small molecules of both endogenous and synthetic origin could dramatically affect the structure of AMPs, which might potentially alter their mechanistic function including antimicrobial efficiency.[5a, 9] Related, it has also been observed that several disordered AMP and protein sequences adopt an ordered secondary structure induced by the lipid mediator lysophosphatidic acid[10] indicating that presence and use of such interactions may be widespread in organisms, a phenomenon far from being understood.

To shed more light on this issue, our present study has focused on CM15, a short, linear, natively unfolded, synthetic hybrid AMP combined from the silk moth cecropin A and the bee venom peptide melittin. CM15 displays a potent broad-spectrum antimicrobial activity retaining the bactericidal effect of cecropins but lacking the strong haemolytic property of melittin.[3, 5a, 5c, 9] With a total charge of +6, it has a much higher average charge per residue than its congeners. The highly cationic N-terminal and a mostly hydrophobic C-terminal region separates to a hydrophilic and a hydrophobic part upon helix formation (**Scheme 1**) coupled to membrane interaction. Based on the above, CM15 was used as model peptide for preliminary screening of folding inducer effect of anionic drugs and biomolecules.[5a] Among the biomolecules and synthetic compounds tested on CM15, the therapeutic drug suramin was the most potent helix promoter,[5a] thus it was selected for this study as the most suitable candidate to address the more complex AMP-small molecule-lipid bilayer interactions. Suramin is a symmetrical, hexasulfonated naphthylurea used as anthelmintics treating onchocerciasis (African river blindness)[11] and sleeping sickness (African trypanosomiasis)[12] since 1920.[13] Suramin also shows anticancer and antiviral properties.[11a, 14]

10.1002/cbic.201800801

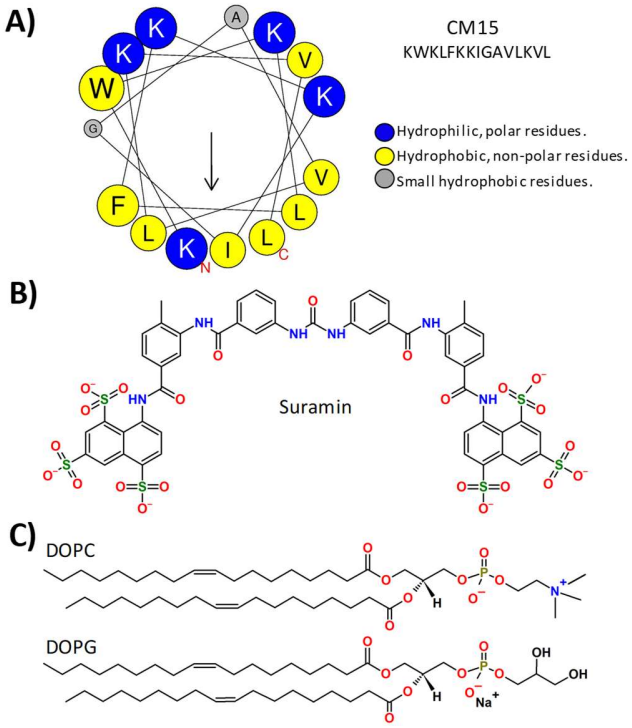

Scheme 1. Structures of the compounds used in the study. **A)** Helical wheel diagram of CM15 (KWKLFKKIGAVLKVL-amide), N and C stand for N- and C-terminus of the peptide, respectively. The helix plot was drawn using HELIQUEST.[15] **B)** Chemical structure of suramin. **C)** Chemical structures of the lipid components used in model membranes built up of dioleoyl-phosphatidylcholine (DOPC) and dioleoyl-phosphatidylglycerol (DOPG). For mimicking mammalian and bacterial cell membrane, pure DOPC and DOPC/DOPG (80/20 n/n%) referred as PC and PC/PG, respectively, were used thoroughly in the study. In the chemical structures, oxygen (O) and nitrogen (N) atoms are colored by red and blue, highlighting negatively and positively charged parts, respectively.

Utilizing *in vitro* binding and functional assays, we characterized the interaction network of the CM15-suramin-membrane system. Results indicate that the drug affects not only the secondary

10.1002/cbic.201800801

structure of the AMP but also its membrane activity, which finally results in decreased antibacterial activity. This observation proposes that so far undetected side effects may be identified when drugs with similar characteristics are administered. Alternatively, the gained insight is also hoped to provide a potential point to exploit towards development of new strategies, where AMP function may be altered or even increased in a controllable manner.

Results and Discussion

Structural changes of CM15 in the presence of suramin and liposomes studied by circular dichroism (CD) spectroscopy

As previously reported,[5a] the drug molecule suramin (Sur) has proven as effective folding inducer of the disordered membrane-active peptide CM15. To understand the structural effect of suramin on the interaction of CM15 with membranes, CD spectra were collected in the presence of the interacting partners.

The far-UV CD spectrum of free CM15 measured in buffer with a sole negative band at around 198-200 nm and no remarkable shoulder in the 210-230 nm region indicates an intrinsically disordered state (**Figure 1A**), which is in agreement with reported observations.[5a, 16] Based on the results presented here and in previous studies,[5a] suramin triggers the disorder-to-order conformational transition of CM15. The characteristic positive-negative couplet corresponding to π-π^* transitions at 195 and 208 nm as well as the negative band at 222 nm of the n-π^* transition (**Figure 1A**) suggest the α-helical folding of CM15.[17] Secondary structure analysis also indicates increased helix content (**Table S1**).[5a] These spectral transformations occurred promptly after addition of the drug and are related to rapid interaction.

Moreover, the relatively low CD signals might be indicative of complex formation accompanied by aggregation, which has been verified by dynamic light scattering (DLS) measurements detecting particles in the micrometer scale.[5a] It is to be noted that the intensity ratio of the CD values at 222 and 208 nm is below ~0.9 for non-interacting α-helices. In line with CD data, this value is >1 for the CM15-suramin mixture (**Figure 1A**) suggesting oligomerization of the peptide

chains. Considering the net charge of +6 and -6 of CM15 and suramin, respectively, neutral 1:1 complexes can easily assemble to higher oligomers or aggregates as suggested previously.[5a]

Structural order gained upon interaction with membranes was probed with PC and PC/PG liposomes mimicking electrostatic features of mammalian and bacterial biomembranes, respectively. Addition of neutral PC liposomes to CM15 renders the main negative band of the peptide to be red shifted (from 198 to 203 nm) associated with intensity decrease and the unresolved negative shoulder at 222 nm more pronounced (**Figure 1A**). This partial helical folding may be the result of a weak, rather hydrophobic interaction lacking electrostatic attraction between the zwitterionic lipids and the peptide.[5b] The outer leaflet of mammalian cell membranes is exclusively composed of neutral, zwitterionic phospholipids, for which charged peptides like CM15 show lower affinity,[18] that is also why ionic AMPs are less toxic towards mammalian cells.[4c, 8b, 8c] In contrast, upon addition of negatively charged PC/PG liposomes, the ID peptide folds into a definite helical conformation (**Figure 1A**). Helix formation is also supported by the estimated ~40% helix content for the lipid-loaded CM15 (**Figure 1B** and **Table S1**). In this case, the driving force of the folding could be the combination of electrostatic interactions between the positively charged residues of the peptide and the negatively charged PG head groups, as well as hydrophobic interactions between the non-polar side chains and the hydrophobic core of the lipid bilayer.[5b, 18]

To test the effect of suramin on lipid-bound peptide, titration with the drug was carried out in the presence of model membranes. Compared to the results obtained for the free peptide where addition of the drug resulted in elevated helix content saturated at 1:1 molar ratio, suramin-dependence was remarkably different (**Figure 1B**). With increasing suramin concentration, the helix content first reduced below the value of the lipid-free state for both vesicles, which was then

followed by a signal increase resulting in approximately doubled helix fraction at 1:2 molar ratio compared to the no suramin state (**Figure 1B**). However, differences between the two liposomes were also revealed. For the neutral PC system, the helical content rises at high suramin ratios (> 60 μM, **Figure 1B**). The phenomenon could be explained in terms of non-specific association of suramin above a threshold concentration on the lipid bilayer rendering the neutral surface negatively charged, which may facilitate peptide binding and induce helical folding. It should be noted that titration curves following the same trend were obtained in the presence and absence of sulfate ions resembling drug sulphonate groups (**Figure 1B**). Thus, it is evident that the sulfate moiety alone is not enough to trigger peptide conformational changes induced by suramin where relative spatial arrangement of the negatively charged groups as well as the separating rings act in concert.

Altogether, these findings suggest that suramin interacts with CM15 even in the presence of lipid bilayers, and control peptide conformation in a concentration-dependent manner. Considering peptide structural changes as well as charge neutralisation effects, mixtures with peptide:suramin ratios of 1:1 and 1:2 were investigated throughout this study.

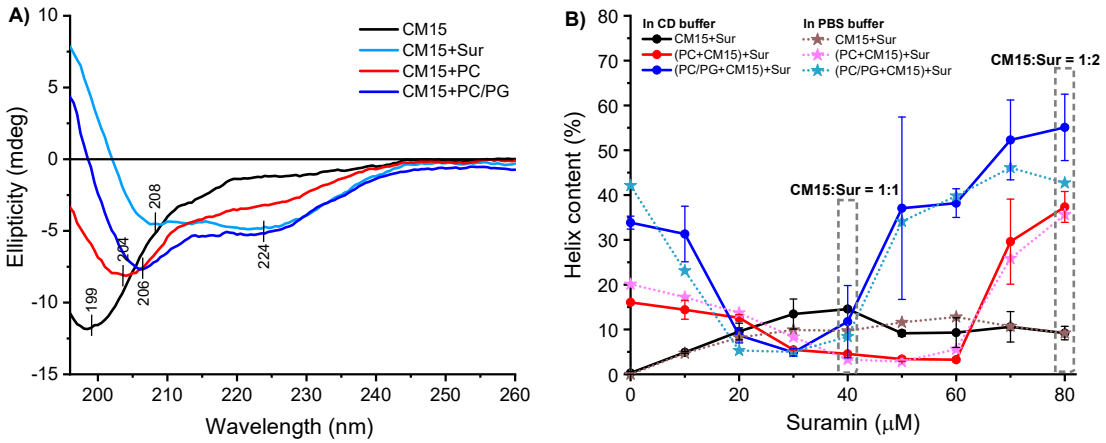

Figure 1. Structural changes of CM15 in the presence and absence of model membranes and suramin studied by CD spectroscopy. **A)** Far-UV CD spectra were taken at peptide, suramin and lipid concentrations of 40, 40, and 635 μM, respectively. **B)** Effect of suramin on the helix content of free and membrane-bound CM15. The peptide (40 μM) was titrated with suramin in the absence and presence of liposomes (635 μM total lipid) using CD buffer or PBS (for the composition see Experimental section). Helix content was estimated using the BestSel online tool.[19] Data are mean±SEM, two series of titrations were carried out using CD buffer, and a single titration was performed in PBS as a control.

To determine relative affinity of the peptide to lipid and small molecule binding partners, three-component mixtures differing only in the order of mixing of the components were tested. In general, spectral features of the liposome-containing samples resemble more those of suramin-loaded peptide than those of the lipid-bound state, and indicate random coil-to-helix transition (**Figure 2** and **Table S1**). However, clear differences could be experienced, which might be attributed to the binding preference of the peptide. For systems with CM15:suramin ratio of 1:2 (**Figure 2B** and **2D**), comparable spectra were obtained for the two-component CM15-suramin complexes and the three-component mixtures where the peptide competes for the partners, (Sur+lipid)+CM15, suggesting the prevalence of peptide-drug binding over the lipid interaction. However, the highest signal exceeding intensities for the pure CM15-suramin complex is detected with PC/PG liposomes when adding suramin to the lipid-bound peptide (**Figure 2D**), which argues for the highest apparent ordered peptide fraction with possibly the lowest level of aggregation for the (CM15+PC/PG)+Sur mixture. This also points to the ability of suramin to enhance helical conformation even when the peptide is already attached to the lipid bilayer. Alternatively, variations in the spectral intensity might be coupled to aggregation induced by the small molecule. In line with these, although the helical character of the peptide is clear, the intensity of the CD

10.1002/cbic.201800801

signal is rather low for most of the three-component mixtures but especially with 1:1 CM15:suramin ratio (**Figure 2A** and **2C**), which could be indicative of higher levels of aggregation.

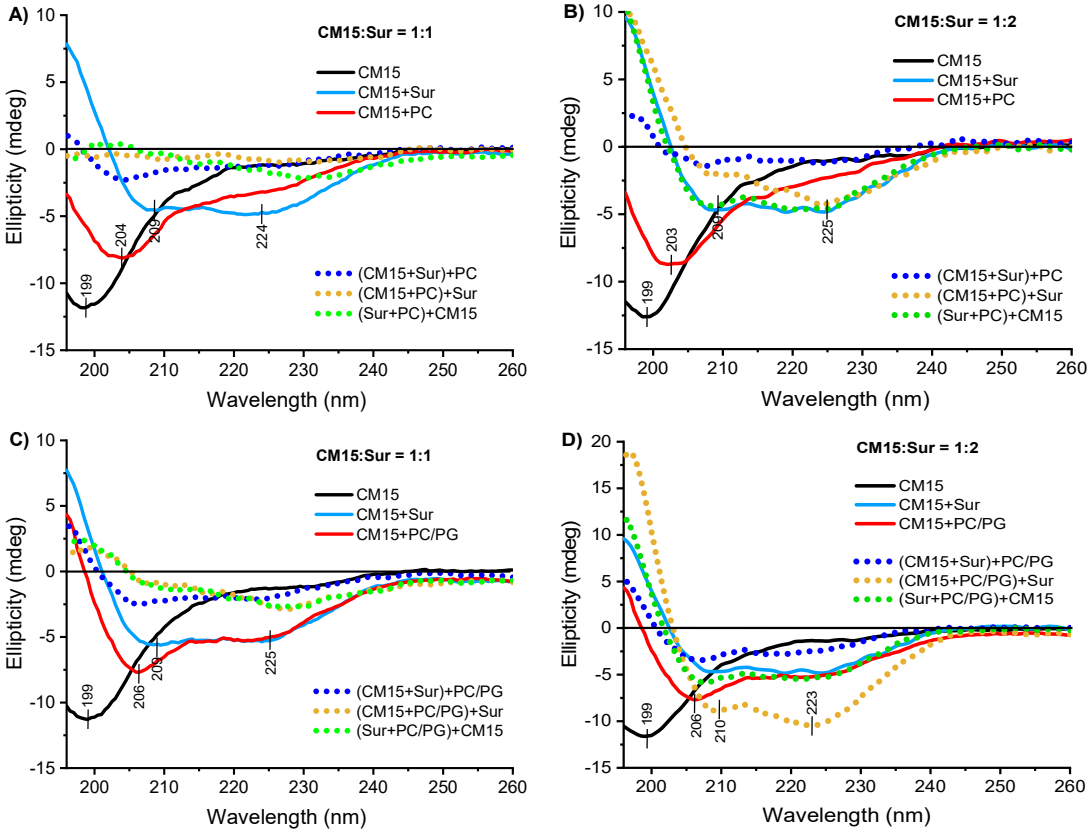

Figure 2. Far-UV CD spectra of CM15 in the presence and absence of model membranes and suramin. Spectra were collected at 40 μM peptide with and without PC (**A** and **B**) or PC/PG (**C** and **D**) liposomes (635 μM total lipid) at CM15:suramin ratios of 1:1 (**A** and **C**) or 1:2 (**B** and **D**). The order of addition in the three-component system was varied so that primarily the preincubation of two compounds in parenthesis was performed, to which than the third compound was added.

Based on CD spectral features observed for the two- and three-component systems, additional information about peptide binding characteristics could be derived. The π-π* band minimum of

the PC/PG-bound CM15 is below 210 nm whereas it is at around 210 nm for the suramin-associated peptide (**Figure 2C** and **2D**). This wavelength shift could reflect polarity changes in peptide backbone surroundings. Specifically, hydrophobic environment provided by PC/PG liposomes could rise the excitation energy of the π-π^* transitions resulting in blue shift. Conversely, the more polar aqueous phase around the CM15-suramin complexes could cause red shift of the π-π^* peak. Based on this consideration, spectral features witnessed for three-component mixtures showing non-reduced signals (**Figure 2B** and **2D**, (Sur+lipid)+CM15 and (CM15+PC/PG)+Sur) are consistent with a binding scenario where peptide chains are not inserted into the apolar interior of the lipid bilayer but rather exposed to the bulk aqueous phase. Furthermore, considering suramin association to the vesicles as suggested above, peptide-suramin interaction might occur at the liposome surface.

CM15-suramin complex aggregation revealed by dynamic light scattering and electron microscopy

To monitor formation of molecular aggregates, dynamic light scattering (DLS) measurements were conducted. As previously indicated,[5a] large associates appeared for the two-component CM15-suramin system with a hydrodynamic diameter in the low micrometer range, which was also confirmed here for both 1:1 and 1:2 peptide:suramin ratios (**Figure 3**, **Table S2** and **S3**). The phenomenon was explained by the mutual charge neutralization within complexes composed from the cationic CM15 and its anionic partner resulting in less hydrophilic adducts prone to aggregation in aqueous environment.[5a]

Peptide binding to the lipids induces no detectable changes in the correlation function so that liposome size of 100 nm was determined for the vesicle-peptide mixtures. Similarly, addition of

suramin to the model membranes caused no perturbation of the curves. However, for the three-component systems, a shift of the correlation function to higher decay times agrees with formation of aggregates with a size greater than 100 nm. The estimated aggregate size in the high nanometer-low micrometer range is similar to that measured for CM15-suramin complexes. Large-sized associates were clearly detected in the presence of PC liposomes but were not so pronounced with PC/PG liposomes. In general, mixtures of preincubated peptide and drug followed by addition of

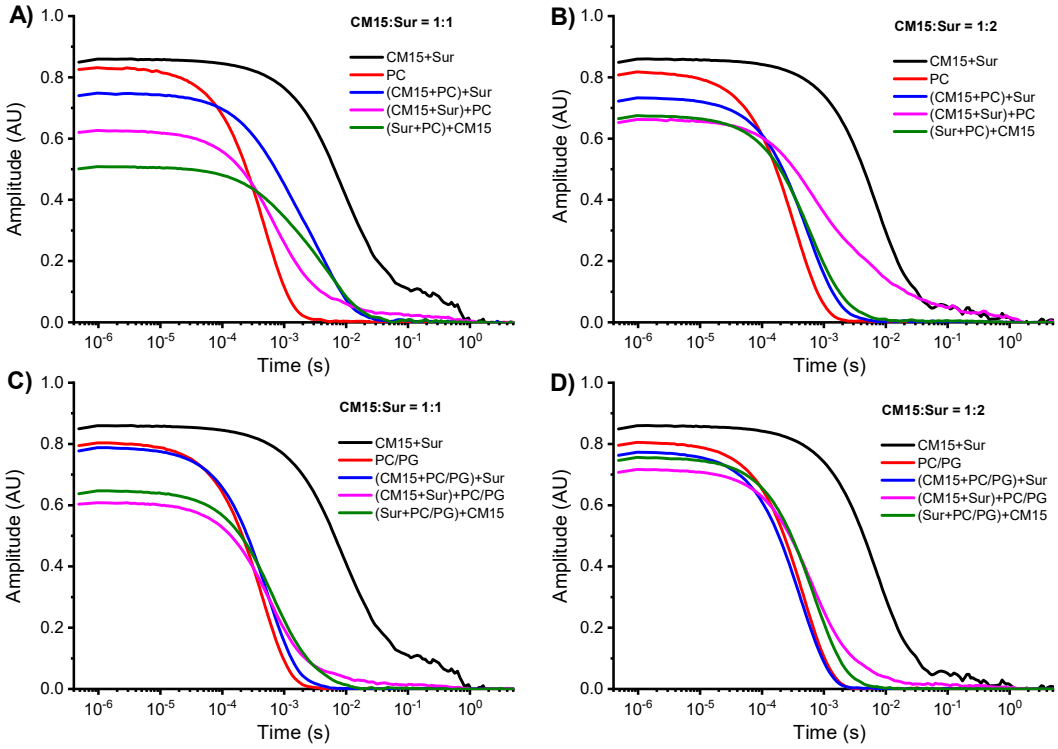

Figure 3. Peptide-drug assembly in the two- and three-component systems monitored by dynamic light scattering. Correlation functions are shown for mixtures with CM15:suramin ratio of 1:1 (**A**, **C**) and 1:2 (**B**, **D**), in the absence and presence of PC (**A**, **B**) and PC/PG (**C**, **D**) liposomes, respectively. Peptide, suramin and lipid concentration is 20, 20 or 40, and 635 μM, respectively. For more details see **Table S2** and **S3**.

lipid vesicles showed the highest propensity to form large aggregates. As an exception to the latter, all three-component systems displayed high-sized particles in the presence of neutral PC liposomes highlighting the importance of peptide-drug charge neutralisation in effective assembly. The association process is also regulated by the CM15:suramin ratio as the size distribution of the aggregates was found to be narrower in the case of the 1:2 ratio compared with the 1:1 (**Table S2** and **S3**). In line with this consideration, no such dependence on the molar ratio was observed for anionic PC/PG vesicles.

Aggregate formation was further investigated by transmission electron microscopy (TEM), providing additional information on the morphology of the CM15-suramin complex. In agreement with DLS results, TEM micrographs for both 1:1 and 1:2 peptide:drug ratios (**Figure 4**) showed formations of up to 1-2 μm diameter with a characteristic morphology. These displayed a network of sphere-like building blocks of ~50 nm interconnected by rather linear regions. Similar associate state depicted as *beadlike branched morphology* was reported for the anticancer/antimicrobial peptide LL-37 in complex with self-RNA as detected by phase contrast light, scanning electron and confocal fluorescence microscopy.[20] These findings suggest that cationic amphiphilic peptides like CM15 and LL-37 might easily form complex aggregates with anionic partners bearing aromatic rings with limited structural flexibility, such as drugs or nucleotides. It should be noted that particles with this morphology are typical for the CM15-suramin complex and were observed neither for sole peptide nor for sole drug solutions.

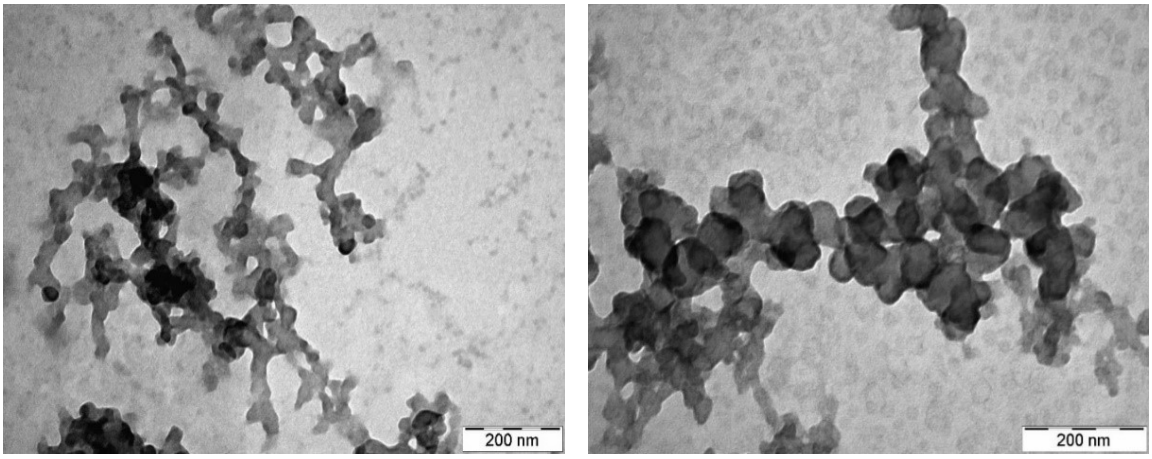

Figure 4. Morphology of the CM15-suramin complex imaged by transmission electron miscoscopy. Micrographs of the mixtures stained with phosphotungstic acid were taken at CM15:suramin ratio of 1:1 (left panel) and 1:2 (right panel). Peptide and suramin concentration in the solution prior drying was 20, and 20 or 40 μM, respectively.

Tryptophan fluorescence indicates altered environment in different lipid complexes

To obtain additional information on the CM15-suramin interaction in the presence of various lipid bilayers, fluorescence spectroscopy measurements were performed. Herein we exploited the intrinsic tryptophan (Trp) fluorescence of the peptide, which sensitively reports a binding event leading to polarity changes in local fluorophore environment.

The spectrum of the free peptide is characterized by an emission maximum at 357 nm (**Figure 5**) in agreement with a water accessible tryptophan of a disordered peptide. Upon addition of the liposomes, the membrane-bound state was easily detected by the blue shift of the maximum. This phenomenon is typical for a peptide tryptophan inserted in a more apolar environment shielded from the aqueous phase. The effect was more pronounced as accompanied with significant intensity increase in the case of the negatively charged PC/PG liposome. In contrast, the rather wide maximum for the PC-bound peptide suggests the co-existence of two tryptophan populations

with different environments. These results agree well with stronger peptide binding connected to a more intimate interaction with PG-containing bilayers compared to the neutral PC liposome, and are also in line with CD-based considerations above.

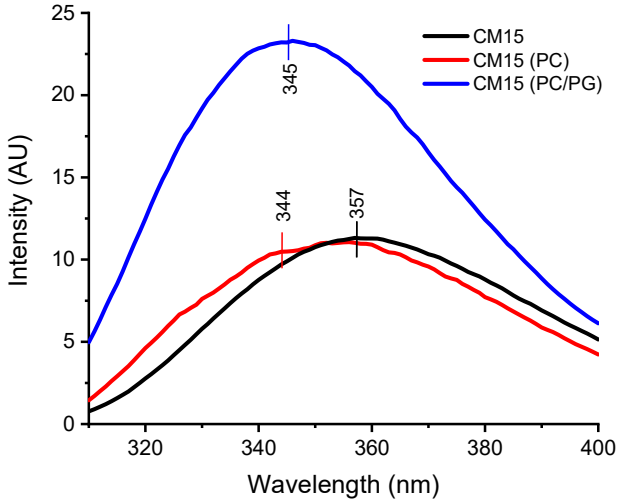

Figure 5. Fluorescence emission spectra of CM15 in the absence and the presence of model membranes. Peptide and lipid concentration were 1 and 100 μM, respectively.

Titration of CM15 with suramin resulted in reduced emission intensity indicating a nearby quencher group in the complex (**Figure 6A**). Considering suramin structure (**Scheme 1**), the aromatic naphtyl moieties could account for the effect, though ligand binding induced helical folding could also lead to tryptophan quenching due to the enhanced rigidity and closer proximity of adjacent side chains.[21] Nevertheless, the moderate dose-dependent intensity decrease leading to almost complete fluorescence loss at 50 μM drug concentration (**Figure 6A**) is characteristic for the CM15-suramin interaction. Similarly, nearly complete loss of fluorescence upon addition of suramin was reported for the recombinant prion PrP protein, which was attributed to suramin-induced aggregation,[22] a phenomenon also detected here for CM15 as discussed above.

For comparison, the same experiment was carried out with the non-binding tryptophan control N-acetyl-tryptophanamide (NATA) which does not form stable complexes with suramin, consenquently can reflect on dynamic quenching and/or inner filter effects. In this case (**Figure 6B**), intensity loss was much weaker, and the lack of static binding of NATA to liposomes or suramin is evident from the slight linear suramin-dependent intensity decrease, which occured to the same extent in the presence and absence of lipid vesicles. Thus, the difference in quenching efficiency comparing the effect of suramin on NATA and CM15 could account to the peptide binding of the drug.

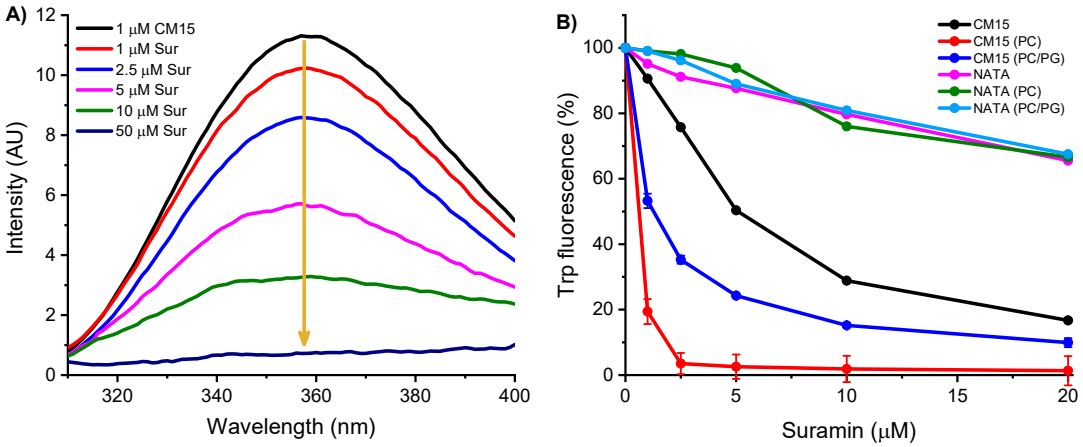

Figure 6. Suramin binding to CM15 in the absence and presence of liposomes studied by peptide fluorescence. **A)** Fluorescence emission spectra of CM15 (1 μM) upon addition of suramin. Arrow indicates increasing drug concentrations. **B)** Normalized maximal emission intensities of CM15 (1 μM) and the control NATA (1 μM) as a function of suramin concentration. Note that error bars for the peptide titration points are mostly smaller than symbol size (data are mean±SEM, n=2).

Performing suramin titration on lipid-loaded peptide, a more effective quenching compared to the lipid-free state was observed suggesting different peptide-drug binding mode (**Figure 6B**). For the PC system, the fluorescence loss was ~85% at 1:1 and was complete at 1:2.5 peptide:suramin

ratio. PC/PG liposomes showed an intermediate behaviour closer to the free peptide than to the PC-bound state. A possible explanation for the phenomenon could be the binding of suramin to the lipid bilayer separately from the peptide and/or to the vesicle-bound peptide resulting in improved relative position of the putative suramin quencher group to access peptide fluorophore. Supposing suramin naphthyl groups as quencher, more efficient quenching detected for PC-bound peptide would require Trp situated closer to suramin and/or in a more suitable relative orientation of the two rings on the two molecules enabling better contact compared to the pure peptide-drug complex. This could relieve some lifting out of the lipid-loaded peptide inserted to some depth into the bilayer, which could be easier for the PC-bound peptide having a looser contact to the vesicle. In contrast, Trp of the peptide bound tighter to PC/PG liposome could remain more incorporated, however, still located closer to the suramin quencher part. For the latter, drug binding is probably less favoured due to the electrostatic repulsion between the negatively charged suramin sulphonyl and PG head groups. Nevertheless, this binding mode assumes preferred interaction of the N-terminal part of CM15 with the middle part of suramin (see **Scheme 1**) in the CM15-suramin complex, which was indeed predicted using computational approach in our group (published separately). Moreover, similar binding characteristics including membrane-associated drug could be deduced from CD findings (see above) and from IR spectroscopy experiments (see below).

Although the ability of suramin to quench a fluorophore like tryptophan has been demonstrated here and reported in the literature,[22] suramin has also intrinsic fluorescence properties related to its naphtylamide moiety. When excited separately from tryptophan at 315 nm, suramin emission with a maximum near 400 nm showed remarkable enhancement of up to 10-fold in the presence of protein binding partners.[23] However, when excited at 295 nm, the wavelength used here for

exciting tryptophan, the weak emission peak developing at ~400 nm showed no sensitivity on drug interactions with CM15 or vesicles (data not shown).

Summarized, fluorescence data suggest perturbed CM15-suramin interaction with different relative conformation of the peptide towards the binding partners in the presence of lipid bilayers. Titration results on lipid-bound CM15 are not compatible with simple peptide displacement by suramin from the vesicles.

Peptide partition between liposome-bound and suramin-complexed states suggested by IR spectroscopy

The interaction between CM15 and lipid assemblies like vesicles has been studied by several groups exploiting IR spectroscopy.[2d, 24] Bastos *et al*.[24d] investigated the interaction between CM15 and liposomes formed from shorter and saturated PC/PG lipids compared to the ones used here. Following lipid carbonyl stretch as a function of increasing peptide concentration, it was reported that the bilayer retained a remarkable order in the presence of the peptide.

Parts of IR spectra involving lipid carbonyl (around 1735 cm^{-1}) as well as peptide amide I (around 1660 cm^{-1}) and amide II (around 1545 cm^{-1}) bands of CM15-liposome associates (**Figure 7A**) were analysed. No drastic changes were observed regarding the lipid order in the bilayer. The small shift of lipid carbonyl bands (from 1736 to 1735 cm^{-1}) in the presence of the peptide suggests that the polar-apolar interface of lipid bilayer could be involved in the interaction with both PC and PC/PG vesicles. More pronounced changes were witnessed in the amide I band of the peptide upon lipid binding. Beside the main band at 1660 cm^{-1} assigned to unordered/helical fraction, a new band component appeared at around 1684 cm^{-1} in the presence of liposomes. In an early study on interaction of melittin and melittin fragments with PC vesicles, Brauner *et al*. [25] observed very

similar spectral feature. They speculated that the band at 1685 cm^{-1} arose from peptides assembled at the lipid surface in an extended conformation.[25] In general, there are controversial results available for CM15 and other membrane-active peptides considering peptide orientation relative to the bilayer, arguing that perpendicular insertion connected mainly to pore formation of the surface-associated peptide might occur above a threshold peptide concentration and peptide:lipid ratio.[3, 5c, 24d]

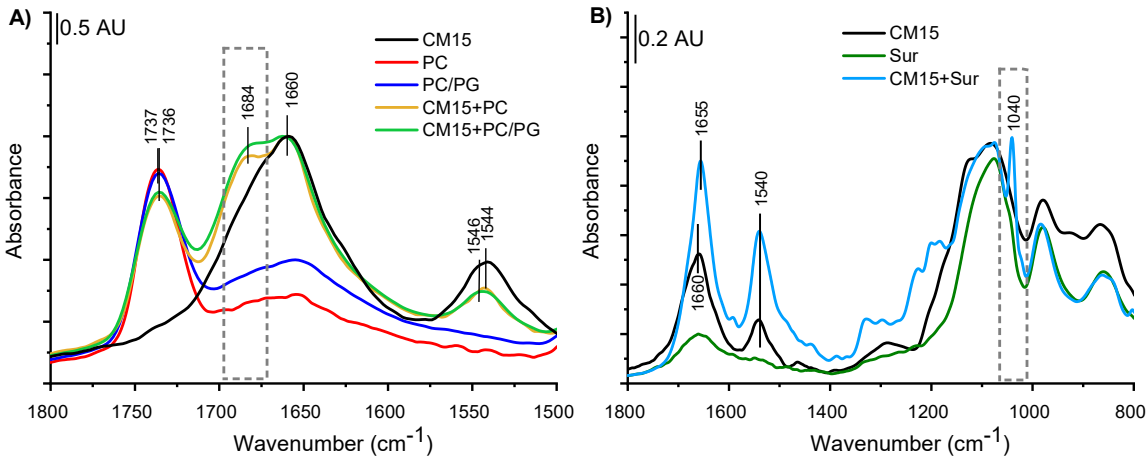

Figure 7. CM15 binding to model membranes and suramin studied by IR spectroscopy. **A)** Amide I and II regions as well as lipid carbonyl band recorded for the CM15-liposome systems. **B)** Formation of CM15-suramin complex indicated by the appearance of an extra band at 1040 cm^{-1}.

The structural changes associated with CM15-suramin interaction can be monitored by means of IR spectroscopy as well (**Figure 7** and **8**). An important advantage of the method is that the signal is not complicated by spectral perturbations due to the presence of aggregates. Changes in the amide I and amide II bands (**Figure 7A**) suggest a protein-like complex structure with predominant helical conformation (corroborated by the amide I peak centred at 1655 cm^{-1}) connected to the suramin induced oligomerization/aggregation. Similar observations were made

10.1002/cbic.201800801

by other methods as well.[5a] In addition, a remarkable feature of the suramin-CM15 complex is the sharp peak at 1040 cm^{-1} that is markedly separated from the buffer phosphate vibrations (**Figure 7B**). This band can be assigned to the in phase S-O stretching of the sulphonyl groups in complexed drug molecules as also observed for suramin oligomers.[26] Thus, the extra band at 1040 cm^{-1} could be used as an IR marker for identification and approximate quantification of CM15-suramin complex formation. We have to point out that at suramin concentrations used, 80 and 160 μM, no such local crowding was detected in the absence of CM15. This is in agreement with NMR data arguing for prevalence of monomers at 0.5 mM but oligomerization at 5 mM concentration.[27]

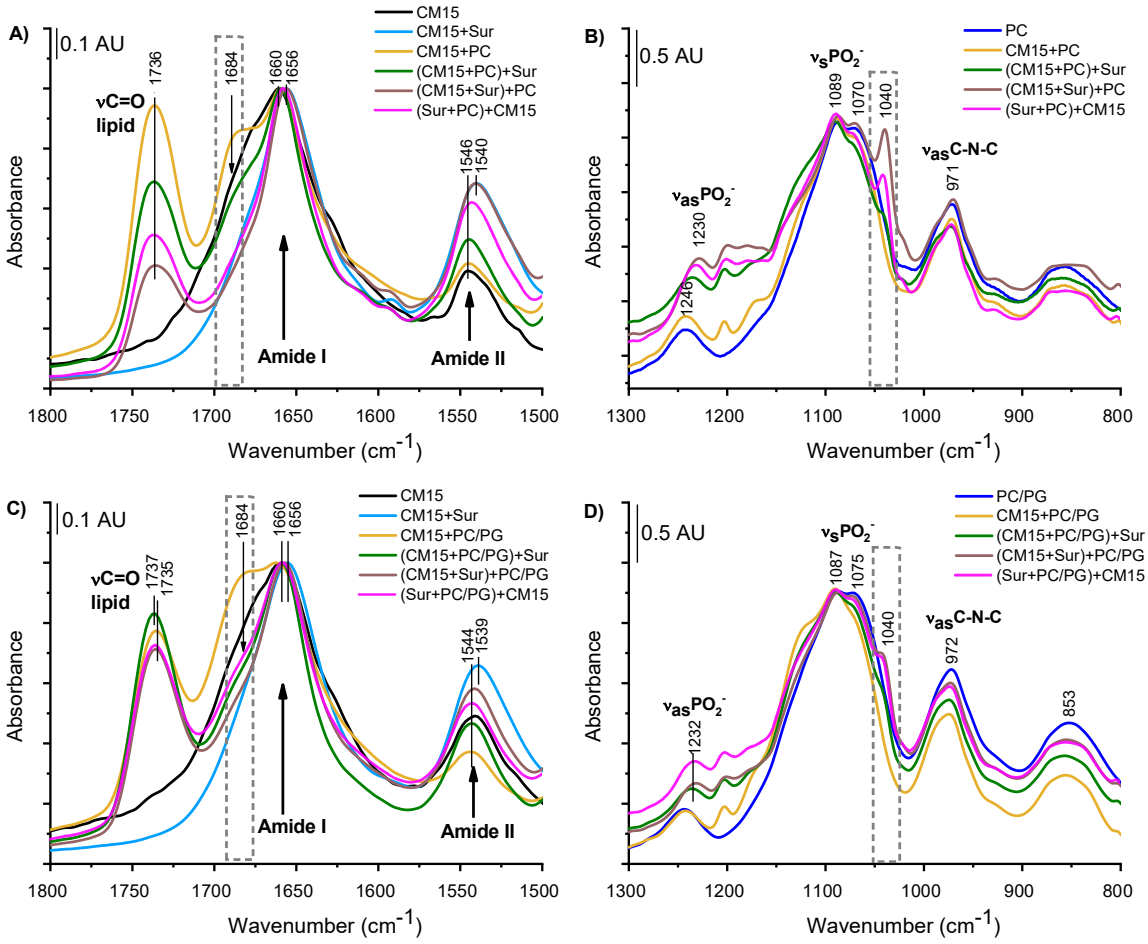

Figure 8. CM15 interactions in the presence of model membranes and suramin studied by IR spectroscopy. (**A**, **C**) Amide I and II regions and lipid carbonyl band. (**B**, **D**) Formation of CM15-suramin complex indicated by the appearance of an extra band at 1040 cm^{-1}. ATR-FTIR spectra were collected for dry films derived from solutions containing CM15 (80 μM), suramin (160 μM) and PC or PC/PG liposome (1.3 mM lipid).

Based on spectral changes experienced for the two-component systems, in the three-component mixtures we focused on the evolution of the amide I band component at 1684 cm^{-1} as well as the band at 1040 cm^{-1}, as a measure of the peptide-lipid and peptide-drug interaction, respectively.

First, liposome systems with 1:2 peptide:suramin ratios were analysed (**Figure 8**), which revealed substantial differences when varying the mixing order of the components. Upon addition of suramin to PC-bound CM15, the intensity of the shoulder amide I band at 1684 cm^{-1} decreases (**Figure 8A**) indicating competition of lipid and drug for the peptide. However, when suramin is added first to CM15 or PC, suppression of the amide I band component is nearly complete (**Figure 8A**) suggesting higher affinity of CM15 towards the drug. Similar trend was observed for the extra band at 1040 cm^{-1} (**Figure 8B** and **Table S4**). According to the band intensity, the highest amount of CM15-suramin complex formed when the peptide and small molecule was mixed first. In case of suramin administration to the PC-bound peptide, the affinity of CM15 towards liposomes is, however, only partially debased, parallel with a reduced CM15-suramin complex formation. When addition of suramin to liposomes was followed by incorporation of the peptide, CM15-suramin complex formation is still remarkable and no redistribution towards liposomes was witnessed. A possible explanation for the latter could be that lipid binding of CM15 is strong enough to interfere with suramin interaction thus the liposome-loaded peptide cannot participate in complex formation with the drug. However, this binding scenario is not in full agreement with CD and DLS results

indicating significant fraction of CM15-suramin associates in the presence of neutral vesicles, which points to a binding event where suramin can interact with liposomes and/or lipid-bound peptide as suggested by CD and fluorescence results. Indeed, liposome-associated suramin causes perturbation of the lipid head group region as indicated by a shift of the lipid asymmetric phosphate vibration (νPO_{as}) at 1240-1250 cm^{-1}.

With reduced suramin concentrations at CM15:suramin ratio of 1:1 in the PC system (**Figure S2**), weaker peptide-liposome interaction was observed for all the three-component mixtures as indicated by the intensity loss of the marker band at 1684 cm^{-1} and the shift of the lipid ester carbonyl band from 1736 to 1737 cm^{-1} (**Figure S2A**). The latter suggests slight lifting of CM15 from the polar-apolar boundary of the bilayer upon suramin addition. On the other hand, the formation of the CM15-suramin complex is less remarkable (**Figure S2B**) compared to the 1:2 CM15:suramin case (**Figure 8B**). Nevertheless, the highest amount of peptide-drug complex is indicated when vesicles were added to the CM15-suramin mixture (**Table S4**).

Using the PC/PG liposome system mimicking the negative charge of bacterial membranes, both similarities and differences were found compared with the neutral PC system. At 1:2 peptide:suramin ratio (**Figure 8**), addition of suramin diminishes the amide I band shoulder at 1684 cm^{-1} significantly but not completely (**Figure 8C**). Furthermore, the marker band of CM15-suramin association at 1040 cm^{-1} (**Figure 8D**) is less pronounced (**Figure 8B**). This is in line with the considerations above, namely that binding of CM15 to negatively charged liposomes is stronger than to neutral lipids, thus peptide-drug complex formation is more hindered in the presence of the former (see also **Table S4**). Based on these results, it can be concluded that in the three-component systems, there is a competition for CM15 between binding to the liposome surface or complex formation with suramin. However, the (CM15+PC/PG)+Sur mixture behaves

exceptionally. For this system, both peptide interactions seem to be diminished according to reduced band intensities at 1685 and 1040 cm^{-1}. Moreover, a slight shift of the lipid carbonyl band from 1735 to 1737 cm^{-1} is observed, which occurs only for this mixture combination.

In contrast to PC/PG liposome systems with 1:2 peptide:suramin ratio, no shift of the lipid carbonyl group was observed for any mixture with 1:1 ratio (**Figure S2C**). Alterations of the 1684 cm^{-1} marker band suggest that in the case of suramin added to the PC-bound peptide, binding of CM15 to the liposome is still strong (**Figure S2C**). Simultaneously, formation of CM15-suramin complex is also hindered as confirmed by the significant intensity loss of the 'complex marker' band at 1040 cm^{-1} (**Figure S2D** and **Table S4**).

To summarize the findings obtained from IR measurements, our results point to dominating peptide-drug interaction when the lipid is added to the preformed CM15-suramin complexes. This preference is stronger at 1:2 CM15:suramin ratio and more relevant for the neutral PC system compared to the charged PC/PG system. Vesicle attachment of CM15 could be strong enough to inhibit CM15-suramin complex formation, however, interaction with suramin could result in peptide lifting from the bilayer interior.

Binding determinants in the three-component systems

Combining the results obtained from the biophysical measurements, we can conclude a general binding scenario in three-component CM15-suramin-lipid systems where CM15 forms complex with suramin in expense to binding to liposomes. However, not all spectral changes observed could be explained by simple peptide displacement. Perturbations in the lipid head group region detected by IR spectroscopy and suggested by fluorescence quenching point to possible suramin binding to the vesicles or even lipid-bound peptide, allowing formation of dynamic complex associates. In

these assemblies, the peptide could be extruded from the polar-apolar boundary of the lipid bilayer but might preserve looser contact with the less buried regime of the lipid head group region facing the aqueous phase.

Moreover, our findings point to the importance of mixing order in peptide binding preference, that is, which binding partner gets in contact with CM15 first. Peptide interaction with the small molecule could dominate over liposome-binding when the lipid is added to preformed CM15-suramin complexes. However, the binding preference is also controlled by peptide:suramin ratio as well as vesicle composition, mainly driven by electrostatics. As CM15 and suramin bears +6 and -6 net charges, respectively, complex formation could be initiated by electrostatic attraction between peptide and drug. In agreement with charge neutralisation at an equimolar ratio and the negative overall charge of the complex at higher suramin ratios, higher peptide partition towards complex formation with suramin leading to more remarkable aggregation was detected at 1:1 CM15:suramin ratio and for the neutral liposome system. In contrast, vesicle attachment of CM15 could inhibit interaction with the drug when suramin meets the peptide associated tightly to the negatively charged membrane.

Our results suggested that electrostatic forces play pivotal role in initiation of peptide binding and assembly. This is consistent with previous studies supposing that electrostatics is a key factor in AMP-membrane interactions.[24d] However, considering the amphiphilic nature of all partners (CM15, suramin, lipids), hydrophobic interactions could also contribute to the binding energetics. Indeed, CD spectra, tryptophan fluorescence and lipid carbonyl vibration indicated peptide regions residing close to the apolar interior of the lipid bilayer. In contrast, CD and IR spectroscopic results suggested more polar environment for suramin-bound CM15 even in the presence of vesicles.

Variations in peptide structure monitored by CD and IR spectroscopy are compatible with a reduced content of the membrane-active peptide conformation in the presence of suramin, which seems to be valid even when considering the ability of suramin to interact with biomembranes. To test the biological relevance of the above interactions and their potential in altering bioactivity, *in vitro* antibacterial and cytotoxicity assays were performed.

Altered antibacterial activity and cytotoxicity of CM15 in the presence of suramin

To understand the biological relevance of the AMP-drug complex formation, antibacterial effect and cytotoxicity on human cells was probed with CM15 premixed with suramin.

On the tested *E. coli* strain, CM15 showed remarkable antibacterial effect as indicated by the fact that no bacterial growth was detected at as low as 5 μM peptide concentration. In the presence of suramin, however, peptide efficiency significantly decreased so that bacterial growth was observed even at higher CM15 concentrations of 10-40 μM (**Figure 9A**). To have a more detailed picture on the effect of suramin, bacteria were treated with 5 μM peptide preincubated with excess suramin. The deep impact of the drug molecule on the antibacterial efficacy of CM15 is evident as significantly higher amount of the bacterial cells survived when CM15 was added with suramin (**Figure 9B**). Furthermore, increasing suramin concentrations resulted in higher relative bacterial growth. Specifically, this value was approximately half at a peptide:suramin ratio of 1:2 compared to that of 1:8 (**Figure 9B**).

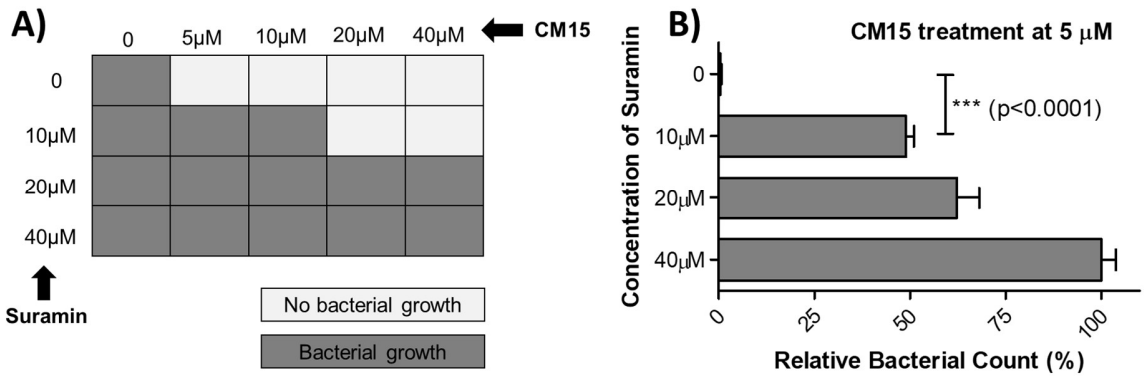

Figure 9. Antibacterial effect of CM15 in the presence and absence of suramin. **A**) *E. coli* treated with peptide-drug mixtures of various ratios. After 24 hrs of incubation, no bacterial growth was detected in the CM15 treated wells. Contrary, when CM15 was added with suramin, visible bacterial growth was observed. **B**) Relative bacterial count after treatment with 5 μM CM15 and various concentrations of suramin. Values are mean±SEM (n=4).

Membrane disrupting activity of CM15 was also tested on human cells, specifically on MonoMac6 monocytes and red blood cells (RBCs). Cells were treated with CM15 in the absence or presence of suramin at 1:1 and 1:2 peptide:suramin ratios. Using the monocyte cell line, CM15 alone was found to be cytotoxic at a relatively low concentration (IC_{50} = 7.6 μM, **Figure 10A**), whereas when administered together with suramin, the effect substantially decreased. Peptide cytotoxicity was impaired to a higher extent at suramin excess (with IC_{50} values of 19.8 and 66.9 μM for the 1:1 and 1:2 ratio, respectively, **Figure 10A**). When treating red blood cells, CM15 alone showed moderate cytotoxicity with a HC_{50} value of ~45 μM (**Figure 10B**), which is in agreement with the reduced haemolytic activity of the hybrid peptide compared to its parent melittin.[28] In the presence of suramin, no haemolysis was observed (HC_{50} > 200 μM, **Figure 10B**). It is to be noted that suramin alone at concentrations up to 100-200 μM showed no effect on these

cells (**Figure 10A** and **10B**), which indicates that reduced peptide cytotoxicity is directly connected to CM15-suramin complex formation.

In an early work, an effective concentration of 10 μM and typical drug dosage of 0.3 mM was reported for suramin.[13] In a recent study, patients were treated with suramin at plasma concentration in the 140-190 μM range and the drug was cleared with a 40 day period half time.[29] As suramin can reach high levels *in vivo*, the interactions investigated here are likely to occur in the human body.

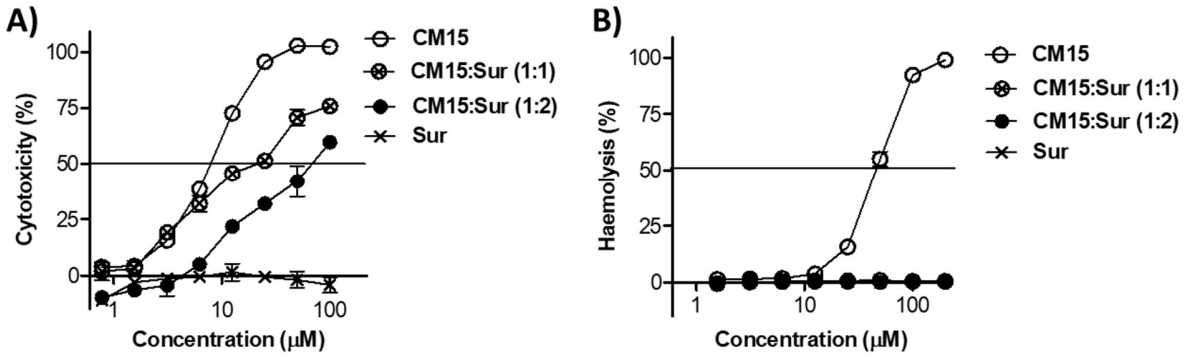

Figure 10. Cytotoxic and haemolytic effect of CM15 in the presence and absence of suramin. Cytotoxicity was measured on MonoMac6 human monocytes and haemolysis was assayed on human RBCs suspension (4 v/v%). Data are mean±SEM (n=3). Note that error bars are often smaller than the symbol size, and the logarithmic scale for the concentration. **A**) Significantly lower cytotoxicity was measured for CM15 administered together with suramin: IC_{50} values for CM15 alone, CM15-suramin at 1:1 and 1:2 ratio are 7.6±0.2, 19.6±4.3, and 66.9±4.5 μM, respectively, with p=0.0011 for CM15 *versus* CM15:Sur (1:1), and p<0.0001 for CM15 *versus* CM15:Sur (1:2), respectively. The effect is higher when CM15 was mixed with suramin at higher (1:2) molar ratio. Suramin alone showed no cytotoxic effect (IC_{50} >100 μM). **B**) Haemolytic activity of CM15 (HC_{50} = 45.9±1.6 μM) was abolished in the presence of suramin at both ratios applied (HC_{50} > 200 μM). Suramin alone showed no haemolytic effect (HC_{50} >200 μM). Note that data points overlap for Sur, CM15:Sur (1:1), and CM15:Sur (1:2).

Concluding remarks

Herein we investigated the structural and functional effects of the therapeutic drug suramin on the membrane-active antimicrobial peptide CM15 by a combination of several biophysical methods. Based on the structural data supported by *in vitro* binding assays, our findings are compatible with a model delineating formation of dynamic complex associates of the peptide populated in lipid-bound and/or drug-loaded forms. CM15 partition is dictated mainly by charge neutralisation effects controlled by suramin-to-peptide ratio and lipid bilayer composition. We also demonstrated that interaction with suramin remarkably changed peptide function as illustrated by significantly reduced antimicrobial activity on Gram-negative bacteria and diminished cytotoxicity towards mammalian cells. Considering the low effective concentration for both CM15 and suramin, high drug plasma levels during medical treatments and locally accumulated AMPs, suramin and AMP levels can fall in the range used in this study. Based on these findings and several other small molecule-AMP interactions demonstrated recently in our group, it is proposed that natural AMPs and host defense peptides will regularly experience alteration of their structure and function in the complex *in vivo* environment – an aspect to be considered and potentially exploited during future treatments and drug design.

Experimental Section

Peptide solution: CM15 was synthesized on solid phase using standard Fmoc/tBu strategy in an automated peptide synthesizer. Peptide product was characterized by analytical RP-HPLC, mass spectrometry and amino acid analysis (see more details in Supporting Information). Lyophilized CM15 powder (trifluoroacetate salt) was dissolved in high purity water at the indicated concentration not higher than 1 mM, aliquoted and stored frozen at -18 ºC until usage no longer than a few weeks.

Suramin solution: Suramin powder (sodium salt, Calbiochem) was dissolved in high purity water at the indicated concentration not higher than 1 mM, aliquoted and stored frozen at -18 ºC until usage.

Lipid solutions: High purity synthetic 1,2-dioleoyl-*sn*-glycero-3-phosphocholine (DOPC) and 1,2-dioleoyl-*sn*-glycero-3-[phospho-*rac*-(1-glycerol)], sodium salt (DOPG) were purchased from the Avanti Polar Lipids Inc. (USA). Liposomes were prepared by using the lipid thin film hydration technique. Lipids were dissolved in chloroform (LabScan, Hungary) containing 50 vol% methanol (Reanal, Hungary), which was then evaporated using a rotary evaporator. The resulting lipid film was kept in vacuum for at least 8 hours to remove residual traces of solvent. The dried lipid film was hydrated with the assay buffer. After repeated heating (37 ºC) and cooling (-196 ºC) steps (at least 10 times), the solutions were extruded through polycarbonate filters with 100 nm pore size (at least 11 times) using a LIPEX extruder (Northem Lipids Inc., Canada). Final lipid concentration was 13 mM. For mimicking mammalian and bacterial cell membrane, pure DOPC and

DOPC/DOPG (80/20 n/n%) referred as PC and PC/PG, respectively, were used thoroughly in the study.

Assay conditions: To mimic physiological conditions, the assay buffer used thoroughly in the study was isotonic phosphate buffered saline (PBS, 10 mM phosphate, 137 mM NaCl, 3 mM KCl, pH 7.4), purchased from Sigma-Aldrich. For measuring CD spectra, a buffer avoiding chloride ions (10 mM Na-phosphate, 100 mM Na_2SO_4, pH 7.0, CD buffer) was used frequently, which allowed spectra collection down to 190 nm.

When investigating three-component systems, the order of addition of the components was varied including preincubation of two compounds (Comp1 and 2) for 3-4 minutes, followed by the incorporation of the third one (Comp3). The corresponding labelling used thoroughly in the text is (Comp1 + Comp2) + Comp3.

Circular dichroism (CD) spectroscopy: CD spectra were collected with a JASCO J-1500 spectropolarimeter at room temperature in 0.1 cm path-length cylindrical quartz cuvette (Hellma, USA). Peptide CD data were collected in continuous scanning mode between 190 and 260 nm at a rate of 50 nm/min, with a data pitch of 0.5 nm, response time of 4 sec, 1 nm bandwidth, and 3 times accumulation. CD curves of peptide, peptide-drug, peptide-liposome and peptide-liposome-drug samples were corrected by spectral contribution of the blank buffer solution. Titration with suramin in the presence and absence of liposomes was performed in duplicate using CD-buffer and as a single experiment in PBS. To estimate secondary structure content of CM15 under various conditions, the software provided by the BeStSel (Beta Structure Selection) website (http://bestsel.elte.hu)[19] was used. Data point are given as mean ± standard error of mean (SEM).

Dynamic Light Scattering (DLS): Mean hydrodynamic diameter (D_h) and polydispersity were measured at 20 °C using a W130i dynamic light scattering device (DLS, Avid Nano Ltd., High Wycombe, UK) with a diode laser (660 nm) and a photodiode detector. Low volume disposable cuvettes with 1 cm path-length were used (UVette, Eppendorf Austria GmbH). Samples containing 20 μM peptide and various amounts of drug and liposomes were measured in a final volume of 80 μl in PBS. The time-dependent autocorrelation functions were measured for 10 seconds, repeated 10 times and the average distributions were reported. The analysis of the measurement data was performed with the iSize 3.0 software, supplied with the device.

Attenuated total reflexion Fourier-transform infrared spectroscopy (ATR FTIR): FTIR spectroscopic measurements were conducted using a Varian 2000 FTIR Scimitar spectrometer (Varian Inc, US) fitted with a liquid nitrogen cooled mercury-cadmium-telluride (MCT) detector and with a 'Golden Gate' single reflection diamond ATR accessory (Specac Ltd, UK). Onto the diamond ATR surface, 5 μl of the sample was mounted and the spectra were collected (2 cm^{-1} resolution and 64 scans) as a dry film (after slowly evaporation of the buffer solvent under ambient conditions). Prior to spectral evaluation, ATR correction was performed and the corrected spectra were smoothed with Savitzky-Golay algorithm (polynomial degree = 2; number of points = 17) using the GRAMS/32 (Galactic Inc., USA) software package.

Fluorescence spectroscopy: Spectra were recorded using a Jobin Yvon Fluoromax-3 spectrofluorimeter (with 3 and 5 nm excitation and emission slits, respectively), at 25 °C in PBS. To test peptide interaction, the tryptophan fluorophore of CM15 was excited at 295 nm and

emission was monitored from 310 to 400 nm. Binding assays were carried out, so as CM15 at 1 μM in the presence and absence of liposomes was titrated with increasing amounts of suramin up to 50 μM. To correct for spectral contribution of the liposomes and suramin, appropriate blank spectra (recorded for solutions containing no fluorophore but lipid and drug at the same concentration) were subtracted. Peptide titrations were performed in duplicate, data presented are mean±SEM.

Transmission electron microscopy (TEM): For direct visualisation of the structure and morphology of the sample, transmission electron microscopy images were obtained using a Morgagni 268D instrument (FEI, The Netherlands). A 2 μl droplet of the sample prepared in PBS was pipetted onto a 200 mesh copper grid with a support film made of formvar, and after 20 seconds contact time, excess liquid was removed. 5% phosphotungstic acid was added immediately as contrast material, then after a contact time of 10 minutes, excess liquid was removed, and the sample was left to air dry.

Antibacterial test, cytotoxicity and haemolytic assay: The antibacterial effect of CM15 in the presence or absence of suramin was measured on *Escherichia coli* strain (DSM 1103). Bacterial lyophilizate were resuspended in Bouillion broth and cultured in blood agar plate for 24 hrs. To test peptide efficacy, 0.5 McFarland standard was diluted 50-times then 100 μl bacterial suspension was plated on a 96-well U-bottom plate. As culture media, Lysogeny broth (LB) was used. CM15 solutions alone or together with suramin were added to the wells in a final concentration of 40, 20, 10, and 5 μM for each compound. Plates were read after 24 hrs of incubation. All samples were measured in quadruplets, data are mean±SEM.

Cytotoxic effect of CM15 was measured on MonoMac6 human monocytic cell line (DSMZ, ACC 124), frequently used and accepted as model cells to assay cytotoxicity, membrane damage, and cellular uptake of compounds like peptides or drugs.[30] Prior to the treatment, cells were cultured in serum-free RPMI-medium and plated (15,000 cells, 100 µl/well) in a flat-bottom 96-well plate. CM15 was dissolved in serum-free medium at a final concentration of 200 µM. Suramin was added to the peptide solution at 1:1 or 1:2 molar ratio. Cells were treated with the serial dilution of CM15 or CM15-suramin mixtures in the concentration range of 0.8-100 µM in quadruplets. Cells were incubated with the compounds for 1.5 h, then cell viability was tested using MTT assay.[31] Briefly, 45 µl MTT (4,5-dimethylthiazol-2-yl)-2,5-diphenyltetrazolium bromide) solution was added to each well (2 mg/ml, solved in serum-free medium). Following 3.5 hrs of incubation, plates were centrifuged at 2000 rpm for 5 minutes, and the supernatant was carefully aspirated with a G30 needle. The precipitated purple crystals were dissolved in 100 µl DMSO, and after 10 minutes agitation, the absorbance was determined at 540 and 620 nm using an ELISA plate reader (iEMS Reader, Labsystems). Cytotoxicity expressed in percentage as a function of peptide concentration was plotted, and IC_{50} values were determined. Data are mean±SEM (n=3).

For haemolytic activity assay, peripheral blood from healthy volunteer (purchased from the Hungarian National Blood Transfusion Service, Budapest, Hungary) was collected in vacuum tubes containing sodium citrate as anticoagulant (Vacuette, 9NC). Tubes were centrifuged (2000 rpm, 5 min) and the pellet was washed twice with PBS. To the pellet, PBS was added to yield a final 4 v/v% RBC suspension. Stock solutions of the compounds were diluted in PBS and two-fold serial dilution series were prepared (final concentration: 1.6 – 200 µM). RBC suspension (100 µl/well) were placed into a 96-well U-bottom cell culture plate and mixed with 100 µl peptide

solution. The plates were incubated for 1.5 hrs at 37°C. After centrifugation (2000 rpm, 5 min), 50 µl of the supernatant was transferred to a flat-bottom microtiter plate and absorbance was measured at 414/450 nm using an ELISA plate reader. Percentage haemolysis is plotted against peptide concentration, and HC50 values (peptide concentration at which 50% haemolysis occurred) were determined. Data are mean±SEM (n=3).

For analyzing statistical significance (p), Student's t-test was performed using GraphPad Prism.

Acknowledgements

This work was supported through the grants provided by the Momentum Program (LP2016-2), the National Competitiveness and Excellence Program (NVKP_16-1-2016-0007), and the GINOP grant (BIONANO_GINOP-2.3.2-15-2016-00017). We also thank for the National Research Development and Innovation Office, Hungary (grants OTKA 104275, 115431, 124077), for grants (VEKOP-2.3.3-15-2017-00020, VEKOP-2.3.2-16-2017-00014) from the European Union and the State of Hungary, co-financed by the European .Regional Development Fund. K. Horváti was supported by the János Bolyai Research Scholarship of the Hungarian Academy of Sciences. Sz. Bősze thanks the ELTE Institutional Excellence Program (783-3/2018/FEKUTSRAT) supported by the Hungarian Ministry of Human Capacities.

References

[1] a) D. Dominey-Howes, B. Bajorek, C. Michael, B. Betteridge, J. Iredell, M. Labbate, *Frontiers in Microbiology* **2015**, *6*; b) Y. Li, Q. Xiang, Q. Zhang, Y. Huang, Z. Su, *Peptides* **2012**, *37*, 207-215; c) K. A. Brogden, *Nature Reviews Microbiology* **2005**, *3*, 238; d) A. Hollmann, M. Martinez, P. Maturana, L. C. Semorile, P. C. Maffia, *Frontiers in Chemistry* **2018**, *6*.

[2] a) Y. J. Gordon, E. G. Romanowski, A. M. McDermott, *Current Eye Research* **2005**, *30*, 505-515; b) R. E. W. Hancock, H.-G. Sahl, *Nature Biotechnology* **2006**, *24*, 1551; c) M. N. Melo, R. Ferre, M. A. R. B. Castanho, *Nature Reviews Microbiology* **2009**, *7*, 245; d) K. N. Alfieri, A. R. Vienneau, C. H. Londergan, *Biochemistry* **2011**, *50*, 11097-11108.

[3] A. Milani, M. Benedusi, M. Aquila, G. Rispoli, *Molecules* **2009**, *14*, 5179-5188.

[4] a) T. Ganz, *Nature Reviews Immunology* **2003**, *3*, 710; b) R. Hancock, A. Patrzykat, *Current drug targets-Infectious disorders* **2002**, *2*, 79-83; c) P. Kumar, J. Kizhakkedathu, S. Straus, *Biomolecules* **2018**, *8*, 4.

[5] a) F. Zsila, S. Bosze, K. Horvati, I. C. Szigyarto, T. Beke-Somfai, *RSC Advances* **2017**, *7*, 41091-41097; b) K. E. S. Locock, *Australian Journal of Chemistry* **2016**, *69*, 717-724; c) S. Pistolesi, R. Pogni, J. B. Feix, *Biophysical journal* **2007**, *93*, 1651-1660.

[6] E. H. Mattar, H. A. Almehdar, H. A. Yacoub, V. N. Uversky, E. M. Redwan, *Cytokine & growth factor reviews* **2016**, *28*, 95-111.

[7] a) S. E. Blondelle, B. Forood, R. A. Houghten, E. Pérez-Payá, *Biopolymers: Original Research on Biomolecules* **1997**, *42*, 489-498; b) H. J. Dyson, P. E. Wright, *Nature Reviews Molecular Cell Biology* **2005**, *6*, 197.

[8] a) M.-A. Sani, F. Separovic, *Accounts of Chemical Research* **2016**, *49*, 1130-1138; b) P. Maturana, M. Martinez, M. E. Noguera, N. Santos, E. A. Disalvo, L. Semorile, P. C. Maffia, A. Hollmann, *Colloids and Surfaces B: Biointerfaces* **2017**, *153*, 152-159; c) T. Shireen, A. Basu, M. Sarkar, K. Mukhopadhyay, *Biophysical chemistry* **2015**, *196*, 33-39.

[9] F. Zsila, T. Juhász, S. Bősze, K. Horváti, T. Beke-Somfai, *Chirality* **2018**, *30*, 195-205.

[10] T. Juhász, J. Mihály, G. Kohut, C. Németh, K. Liliom, T. Beke-Somfai, *Scientific reports* **2018**, *8*, 14499.

[11] a) L. Henß, S. Beck, T. Weidner, N. Biedenkopf, K. Sliva, C. Weber, S. Becker, B. S. Schnierle, *Virology Journal* **2016**, *13*, 149; b) J. E. Allen, O. Adjei, O. Bain, A. Hoerauf, W. H. Hoffmann, B. L. Makepeace, H. Schulz-Key, V. N. Tanya, A. J. Trees, S. Wanji, D. W. Taylor, *PLOS Neglected Tropical Diseases* **2008**, *2*, e217; c) C. P. Chijioke, R. E. Umeh, A. U. Mbah, P. Nwonu, L. L. Fleckenstein, P. O. Okonkwo, *European Journal of Clinical Pharmacology* **1998**, *54*, 249-251; d) B. Thylefors, *Bulletin of the World Health Organization* **1978**, *56*, 63-73.

[12] A. J. Nok, *Parasitology Research* **2003**, *90*, 71-79.

[13] V. Fourneau, Tréfouel, J., & Vallée, J., *Ann. Inst. Pasteur* **1924**, *38*, 81-114.

[14] a) M. R. Mirza, E. Jakobsen, P. Pfeiffer, B. Lindebjerg-Clasen, J. Bergh, C. Rose, *Acta Oncologica* **1997**, *36*, 171-174; b) M. A. Eisenberger, L. M. Reyno, D. I. Jodrell, V. J. Sinibaldi, K. H. Tkaczuk, R. Sridhara, E. G. Zuhowski, M. H. Lowitt, S. C. Jacobs, M. J. Egorin, *JNCI: Journal of the National Cancer Institute* **1993**, *85*, 611-621; c) R. Dreicer, D. C. Smith, R. D. Williams, W. A. See, *Investigational New Drugs* **1999**, *17*, 183-186; d) G. H. Salvador, T. R. Dreyer, A. A. Gomes, W. L. Cavalcante, J. I. Dos Santos, C. A. Gandin, M. de Oliveira Neto, M. Gallacci, M. R. Fontes, *Scientific reports* **2018**, *8*, 10317.

[15] R. Gautier, D. Douguet, B. Antonny, G. Drin, *Bioinformatics* **2008**, *24*, 2101-2102.

[16] R. W. Woody, *Instrumental analysis of intrinsically disordered proteins: Assessing structure and conformation* **2010**, 303-321.

[17] B. Nordén, A. Rodger, T. Dafforn, *Linear dichroism and circular dichroism*, The Royal Society of Chemistry, **2010**.

[18] K. Matsuzaki, *Biochimica et Biophysica Acta (BBA) - Biomembranes* **1999**, *1462*, 1-10.

[19] A. Micsonai, F. Wien, L. Kernya, Y.-H. Lee, Y. Goto, M. Réfrégiers, J. Kardos, *Proceedings of the National Academy of Sciences* **2015**, *112*, E3095-E3103.

[20] D. Ganguly, G. Chamilos, R. Lande, J. Gregorio, S. Meller, V. Facchinetti, B. Homey, F. J. Barrat, T. Zal, M. Gilliet, *The Journal of Experimental Medicine* **2009**, *206*, 1983-1994.

[21] a) A. Ghisaidoobe, S. Chung, *International journal of molecular sciences* **2014**, *15*, 22518-22538; b) J. R. Tusell, P. R. Callis, *Biophysical Journal* **2011**, *100*, 174a.

[22] S. Gilch, K. F. Winklhofer, M. H. Groschup, M. Nunziante, R. Lucassen, C. Spielhaupter, W. Muranyi, D. Riesner, J. Tatzelt, H. M. Schätzl, *The EMBO journal* **2001**, *20*, 3957-3966.

[23] a) S. L. Fleck, B. Birdsall, J. Babon, A. R. Dluzewski, S. R. Martin, W. D. Morgan, E. Angov, C. A. Kettleborough, J. Feeney, M. J. Blackman, A. A. Holder, *J Biol Chem* **2003**, *278*, 47670-47677; b) C. R. Middaugh, H. Mach, C. J. Burke, D. B. Volkin, J. M. Dabora, P. K. Tsai, M. W. Bruner, J. A. Ryan, K. E. Marfia, *Biochemistry* **1992**, *31*, 9016-9024; c) Q. Wu, J. Wang, L. Zhang, A. Hong, J. Ren, *Angew Chem Int Ed Engl* **2005**, *44*, 4048-4052; d) Y. L. Zhang, Y. F. Keng, Y. Zhao, L. Wu, Z. Y. Zhang, *J Biol Chem* **1998**, *273*, 12281-12287.

[24] a) K. Bhargava, J. B. Feix, *Biophysical journal* **2004**, *86*, 329-336; b) H. Sato, J. B. Feix, *Biochimica et Biophysica Acta (BBA)-Biomembranes* **2006**, *1758*, 1245-1256; c) M. Sharon, Z. Oren, Y. Shai, J. Anglister, *Biochemistry* **1999**, *38*, 15305-15316; d) M. Bastos, G. Bai, P. Gomes, D. Andreu, E. Goormaghtigh, M. Prieto, *Biophysical journal* **2008**, *94*, 2128-2141.

[25] J. W. Brauner, R. Mendelsohn, F. G. Prendergast, *Biochemistry* **1987**, *26*, 8151-8158.

[26] a) N. Lehmann, G. K. Aradhyam, K. Fahmy, *Biophysical journal* **2002**, *82*, 793-802; b) M. Y. Skripkin, P. Lindqvist-Reis, A. Abbasi, J. Mink, I. Persson, M. Sandström, *Dalton transactions* **2004**, 4038-4049.

[27] T. Polenova, T. Iwashita, A. G. Palmer, 3rd, A. E. McDermott, *Biochemistry* **1997**, *36*, 14202-14217.

[28] a) P. Juvvadi, S. Vunnam, E. L. Merrifield, H. G. Boman, R. Merrifield, *Journal of peptide science: an official publication of the European Peptide Society* **1996**, *2*, 223-232; b) H. Sato, J. B. Feix, *Antimicrobial agents and chemotherapy* **2008**, *52*, 4463-4465.

[29] C. J. Bowden, W. D. Figg, N. A. Dawson, O. Sartor, R. J. Bitton, M. S. Weinberger, D. Headlee, E. Reed, C. E. Myers, M. R. Cooper, *Cancer chemotherapy and pharmacology* **1996**, *39*, 1-8.

[30] a) H. L. Ziegler-Heitbroc, E. Thiel, A. Futterer, V. Herzog, A. Wirtz, G. Riethmüller, *International journal of cancer* **1988**, *41*, 456-461; b) É. Kiss, G. Gyulai, E. Pári, K. Horváti, S. Bősze, *Amino Acids* **2018**, *50*, 1557-1571; c) K. Horváti, B. Bacsa, T. Mlinkó, N. Szabó, F. Hudecz, F. Zsila, S. Bősze, *Amino acids* **2017**, *49*, 1053-1067.

[31] a) Y. Liu, D. A. Peterson, H. Kimura, D. Schubert, *J Neurochem* **1997**, *69*, 581-593; b) T. Mosmann, *J Immunol Methods* **1983**, *65*, 55-63; c) E. C. Slater, *Ned Tijdschr Geneeskd* **1963**, *107*, 1543-1544.

10.1002/cbic.201800801

Table of Content

Antimicrobial peptides (AMPs) experience a complex environment in their host organisms, which may significantly affect their function. The cationic AMP CM15 forms a tight complex with the polyanionic drug suramin controlling peptide structure upon membrane binding. This case study demonstrates on the three-component system that by modulating AMP structure, its antibacterial activity is also changed.